

RESEARCH ARTICLE

Andrographis paniculata Leaf Extract Increases Interleukin-2 in Malnutrition Rat Model

Fortuna Dwiningsih^{1,*}, Rosdiana Natzir^{1,2}, Ilhamuddin^{1,2}, Ika Yustisia^{1,2}, Sulfahri^{1,3}

¹Master Program of Biomedical Science, Graduate School, Universitas Hasanuddin, Jl. Perintis Kemerdekaan No.Km. 10, Makassar, Indonesia

²Department of Biochemistry, Faculty of Medicine, Universitas Hasanuddin, Jl. Perintis Kemerdekaan No.Km. 10, Makassar, Indonesia

³Department of Biology, Faculty of Mathematics and Natural Sciences, Universitas Hasanuddin, Jl. Perintis Kemerdekaan No.Km. 10, Makassar, Indonesia

*Corresponding author. Email: ddwiningsih24@gmail.com

Received date: Feb 16, 2024; Revised date: May 13, 2024; Accepted date: May 15, 2023

Abstract

BACKGROUND: Malnutrition is a global health concern that results in changes in nutritional status, as indicated by alterations in phenotypic markers, hematological and biochemical parameters, and increased susceptibility to infection, as shown by decreased interleukin (IL)-2 levels. Andrographolide, the active component of *Andrographis paniculata*, stimulates the immune system and exhibits antibacterial and antiviral activity. Therefore, *A. paniculata* may serve as a potential adjuvant therapy for malnutrition. This study was conducted to analyze the effect of *A. paniculata* as an immunomodulator against malnutrition with characteristics of environmental enteric dysfunction (EED) and a low-protein diet by examining phenotypic markers, hematological, biochemical, and IL-2 levels.

METHODS: Forty-five male Wistar rats were divided into seven groups. They were fed either a standard or a low-protein diet before receiving oral administration of various concentrations of *A. paniculata* leaf extract (APLE). APLE was administered 21 days after the initial low-protein diet. Hematological, biochemical, and phenotypic markers were assessed to determine the nutritional status of the rats. The protective effects of APLE were evaluated by measuring IL-2 levels using enzyme-linked immunosorbent assay (ELISA).

RESULTS: Malnourished rats exhibited slow body growth, physical and behavioral changes, reduced leukocyte count, total protein, albumin, cholesterol, and villi length. Malnourished rats treated with APLE showed a more effective and significant increase in IL-2 levels, with higher concentrations of APLE resulting in higher IL-2 levels.

CONCLUSION: APLE, in a concentration-dependent manner, can increase IL-2 levels, suggesting that APLE may have potential protective effects in a rat model of malnutrition.

KEYWORDS: *Andrographis paniculata*, environmental enteric dysfunction, interleukin (IL)-2, low protein, malnutrition

Indones Biomed J. 2024; 16(3): 218-27

Introduction

Malnutrition occurs when macronutrients such as carbohydrates, proteins, and fats, as well as micronutrients such as vitamins and minerals, are not consumed in adequate amounts.(1) By 2022, there were 148.1 million stunted children worldwide. Among them, an estimated 45 million

experienced wasting, with 13.6 million being severely malnourished.(2)

The most prevalent type of malnutrition worldwide is protein-energy malnutrition (PEM), which can be classified into three stages: kwashiorkor, marasmus, and marasmic-kwashiorkor.(3) Previous studies have shown that malnutrition, particularly PEM, leads to global human immunodeficiency and is intimately linked to infections.(4)

Millions of malnourished individuals, primarily youngsters under five years of age, frequently pass away from infections. (5) The host's capacity to fight infection is compromised by low nutrient intake, which also damages innate and acquired immunity and impairs the function of cells and organs. (6) The host's nutritional condition influences its vulnerability to infectious illnesses, hinders nutrient absorption, and exacerbates malnutrition. (4,7) It is crucial to understand how malnutrition aggravates illnesses and how nutrition prevents them because of this inherent relationship and the high mortality rate caused by malnutrition. (8)

Stunting and cognitive deficits are caused by a vicious cycle exacerbated by malnutrition and environmental enteric dysfunction (EED). (9) Among other characteristics, intestinal hyperpermeability inflammation and villus blunting are indicative of malfunctioning of the intestinal barrier that characterizes EED. (10) EED was created using a mouse undernutrition model that triggers the enteric breakdown of the gut barrier. A diet lacking protein causes undernutrition, and indomethacin causes small-intestinal damage. (11)

Malnutrition resulting from dietary restriction and severe hunger is known to cause a series of metabolic changes that lead to reduced body mass, decreased immune function, and alterations in digestive system function, particularly in the liver and small intestine. Biochemical parameters, such as lower glucose, triglycerides, and serum proteins, such as albumin, are commonly used to assess nutritional status. (12) A lack of nutrients, such as proteins, can impair many biological processes, including leukopoiesis, compromising the immune response and resulting in leukopenia. (13) Cytokines such as interleukin (IL)-12, IL-18, and IL-21 play crucial roles in the differentiation of Th1 cells. In malnourished children, the gene and protein expression of these cytokines, as well as the plasma levels of IL-12, are reduced, leading to lower concentrations of interferon (IFN)- γ and IL-2. (14) To address the root causes of malnutrition, interventions should focus on improving nutrition and preventing related diseases. (15) Some herb drugs can be used as alternative treatment against malnutrition and have been studied, among them are *Moringa oleifera*, Spirulina, and bee pollen. Additionally, alternative treatments such as herbal medicines, such as *Andrographis paniculata*, can boost the immune system to protect against infections and prevent the outcome of the worsening of pathophysiological processes.

Several studies reported that *A. paniculata* has the potential as an antimicrobial, regulates the balance of pro-inflammatory and anti-inflammatory immune responses,

maintains host cells to fight infection, reduces drug side effects, and is an alternative therapy to boost the immune system. (16) Andrographolide, a labdane diterpenoid is the most bioactive compound isolated from *A. paniculata*, enhances the proliferation and secretion of IL-2 (17), treatment with andrographolide reduces histopathological alterations in villus height and crypt depth (18). This study was conducted to analyze the effect of *A. paniculata* as an immunomodulator in a model of malnutrition with characteristics of environmental enteric dysfunction (EED) and a low-protein diet by examining phenotypic markers and hematological, biochemical, and IL-2 levels.

Methods

Preparation of Purified *A. paniculata* Leaf Extract (APLE)

A. paniculata plants were purchased from and identified by CV Indonegri (Malang, Indonesia) with specimen No. #23032192890. Simplicia of *A. paniculata* leaves were oven-dried and ground into a fine powder using a grinder. Dried ground powder of *A. paniculata* was extracted by maceration with 95% ethanol and stirred for 24 h. After filtration, the filtrate was collected and the sediment was re-extracted five times. The macerate was filtered using a vacuum pump and evaporated using a rotary evaporator at 40°C to obtain a viscous extract. The ethanol extract was then analyzed using thin-layer chromatography (TLC CAMAG Linomat 5 S/N 210989; Camag, Muttenz, Switzerland) to determine the content of the active compound andrographolide (Cat No. 365645; Sigma-Aldrich, St. Louis, MO, USA). (19)

Malnutrition Animal Model

Forty-five male Wistar rats, aged between 4-5 weeks and with an average weight of 81.6 \pm 2.15 grams were selected from the farm stock. The rats were acclimated with a standard diet and drink for seven days. Every trial was conducted in a climate-controlled space with a 12/12 light/dark cycle. After each experiment, the rats were euthanized by injecting a lethal dose of 1 mg/kg xylazine and 40 mg/kg ketamine intraperitoneally. All protocols for animal handling, management, and slaughtering were authorized by the Health Research Ethics Committee of the Universitas Hasanuddin Teaching Hospital, and Dr. Wahidin Sudirohusodo Makassar Regional General Hospital (No. 58/UN4.6.4.5.31/PP36I2A23).

The diets were provided in pellet form, with the control group and the low-protein group receiving 15 g of rat chow

per day. The composition of the diets was detailed in Table 1.(20) The malnutrition group was fed at varying times each day to induce malnutrition and to prevent the body from adapting to nutritional restrictions. Water was provided *ad libitum* in both experimental groups.

This study was a randomized controlled trial with a post-test control group. Male rats were divided into seven groups each consisting of five rats. Two groups only received treatments for 21 days for the confirmation of the malnourished rats model. Rats in the control group (Control') were fed a standard diet for 21 days. Rats in the malnourished group (2%LP+IND') were fed with low protein 2% for 21 days, added with intraperitoneal injection of 3.5 mg/kgBW/day indomethacin diluted in methyl sulfoxide at day 14–21. Meanwhile the other 5 groups were treated for 42 days. Rats in the control group (Control) were fed a standard diet for 42 days. Rats in the malnourished group (2%LP+IND) were fed with low protein 2% for 42 days, but added with intraperitoneal injection of 3.5 mg/kg BW/day indomethacin diluted in methyl sulfoxide at day 14–21 only. Rats in the 2%LP+IND+AP1 group were fed with low protein 2% for 42 days, added with intraperitoneal injection of 3.5 mg/kgBW/day indomethacin diluted in methyl sulfoxide at day 14–21, followed by 47.25 mg/kgBW/day of APLE given orally at day 22–42. Rats in the 2%LP+IND+AP2 group and 2%LP+IND+AP3 group received similar treatment with 2%LP+IND+AP1 group,

with only difference in the concentration of APLE given, which were 94.5 mg/kgBW/day and 189 mg/kgBW/day, respectively (Figure 1).

Relative Organ Weight and Weight-for-Age (WA) Measurement

The body weights of all rats were measured using a digital scale on days 1, 3, 5, 7, 9, 11, 14, 21, 28, 35, and 42. To analyze the effects of malnutrition on organs, the rats were euthanized, and the spleen and liver were aseptically removed and weighed on a digital scale. The relative organ weight was calculated using the formula: (total organ weight/body weight) × 100.

WA, a scale used to measure malnutrition in mice based on body measurements, can be related to the human scale of malnutrition. The WA calculation in rats, using a malnutrition scale model, involves determining the weight of the rats according to their age, the calculation of the WA in rats involves employing the subsequent equation: (sacrifice weight of the animal in diet group / expected weight based on mice in the control diet) × 100%.(21) Following human classification, the Anstead model suggests that rats with WA values ranging from 76 to 90% can be categorized as experiencing mild malnutrition.(21) Rats with WA values between 61 and 75% were classified as moderately malnourished. Lastly, rats with WA values ≤60% were classified as severely malnourished.

Hematological, Biochemical, and IL-2 Analysis

On days 21 and 42, 1 mL of blood was collected from the subjects via cardiac puncture for hematological, biochemical, and IL-2 analyses. The blood sample was centrifuged at 4000 revolutions per minute to separate the serum. Hematological parameters were measured using a Sysmex KX-21 hematology analyzer (Sysmex Corporation, Kobe, Japan). Both hematological parameters and overall blood cell count were subsequently determined. Biochemical parameters were measured using a Biosystem automatic BA 200 biochemistry analyzer (Biosystems Diagnostic, Popești-Leordeni, Romania). Serum levels of various biochemical parameters, including total protein, albumin, glucose, alanine aminotransferase (ALT), cholesterol, and triglycerides, were then assessed. The methods used to examine total protein were biuret, albumin using bromocresol green (BCG), glucose using GOD-PAP photometric, ALT using IFCC kinetic photometric, cholesterol using (Cholesterol Oxidase Peroxidase Aminoantipirin) CHOD-PAP photometric, and triglycerides using glycerol phosphate oxidase/peroxidase (GPO-PAP) photometric. IL-2 levels were estimated using

Table 1. Composition of the experimental diets.

Nutrient Composition	Standard Diet	Low-Protein
Protein (%)	18.5	2.2
Carbohydrates (%)	38.9	72.3
Fat (%)	2.7	2.7
Metabolizable energy (kcal/kg)	3329	3306
Ingredients		
Rice bran (g)	11	28
Ground corn (g)	18	12
Tapioca flour (g)	10	56
Soybean meal (g)	30	0.5
Fish flour (g)	28	0.5
Crude Palm Oil (g)	1	1
Premix ¹ (g)	2	2
Total (g)	100	100

¹The following nutrients are provided per kg of feed: 24000 IU vitamin A, 4000 IU vitamin D3, 16 IU vitamin E, 4 mg vitamin K, 4 mg vitamin B1, 10 mg vitamin B2, 1 mg vitamin B6, 24 mg vitamin B12, 240 mg manganese, 40 mg iron, 200 mg zinc, 0.4 mg iodine, 12 mg calcium.

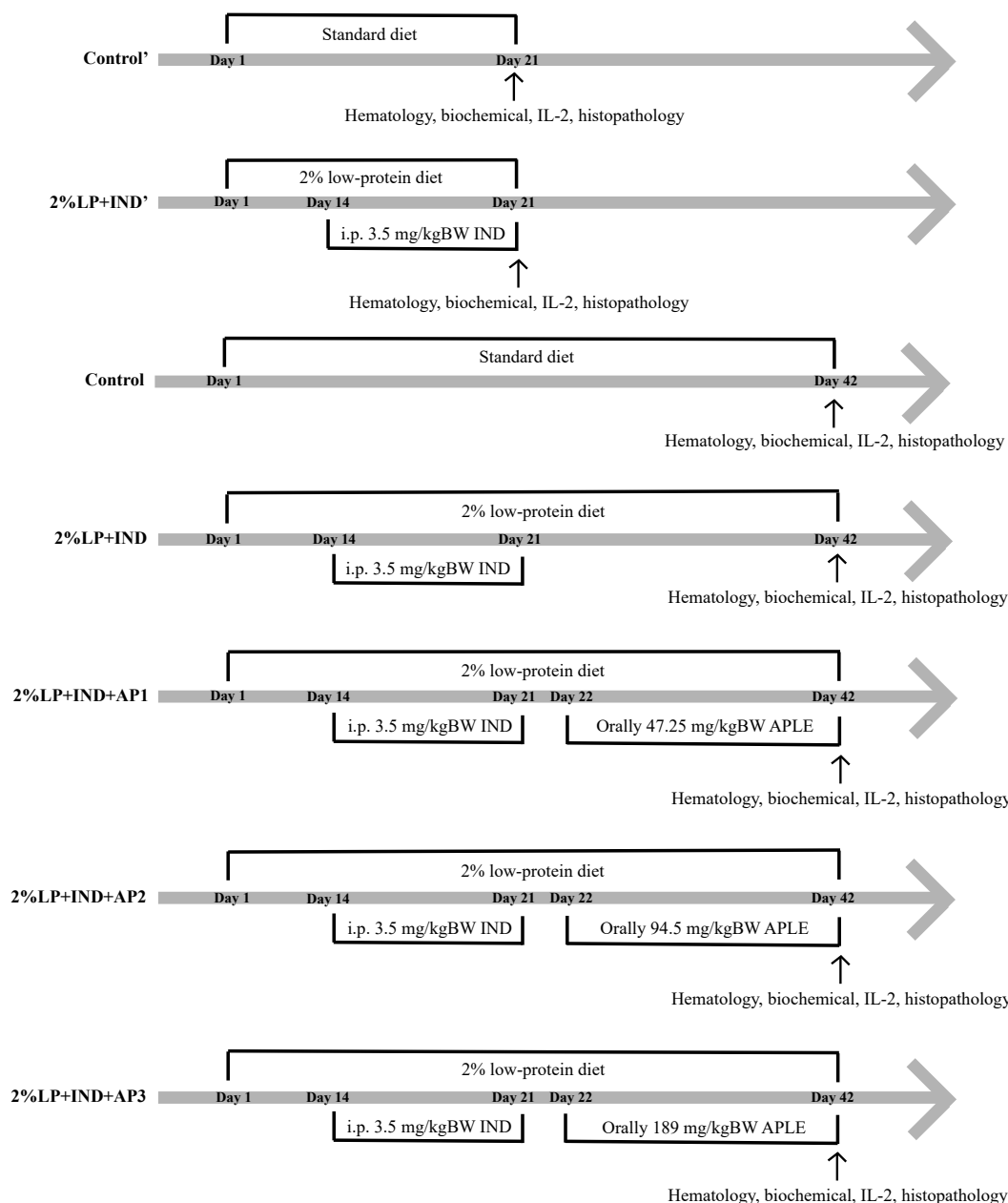


Figure 1. Schematic diagram of the study design and timeline.

a highly specific rat IL-2 enzyme-linked immunosorbent assay (ELISA) kit (Cat. RAB0288; Sigma-Aldrich, St. Louis, MO, USA). Standards and samples pipetted into the wells and IL-2 present in a sample was bound to the wells by the immobilized antibody. The wells were washed, and biotinylated anti-rat IL-2 antibody was added. After washing away unbound biotinylated antibodies, HRP-conjugated streptavidin was pipetted to the wells. The wells were washed, and a TMB substrate solution was added to the wells and color develops in proportion to the amount of IL-2 bound. The Stop Solution changed the color from blue to yellow, and the intensity of the color was measured at 450 nm.

Histology Analysis

Samples of jejunum were embedded in paraffin, and using a microtome 4 µm sections were cut and stained with a hematoxylin-eosin-saffron (HES) solution. Two study blinded-pathologists performed the histopathological examinations. For each stained intestinal tissue section, 5 different areas were selected and documented at 100× magnification under an upright light microscope. Olympus BX53 Digital Microscope (Olympus Corporation, Tokyo, Japan) was used to evaluate the samples. The Olympus cellSens program (Olympus Corporation) was used for the histological examination of jejunal villi height (µm), crypt depth (µm), and jejunal muscular thickness (µm).

Statistical Analysis

All data are presented as mean±SEM. Statistical analyses were performed using GraphPad Prism 9 (GraphPad Software, La Jolla, CA, USA). ANOVA was employed, followed by a Tukey or Mann-Whitney post-hoc test to compare more than two groups, whereas the unpaired t-test was used to compare the means of two groups. Statistical significance was set at $p < 0.05$.

Results

Phenotypic Analysis Results of the Malnutrition Rat Model

At the end of the experiment, rats in the *A. paniculata* treatment groups showed a significant loss of body weight compared to control rats ($p < 0.05$, Figure 2). The spleens

and livers of the rats were aseptically removed and weighed to analyze the effects of malnutrition on organ development. Malnourished rats showed significant differences in spleen weight compared to control rats ($p = 0.0114$). Additionally, malnourished rats exhibited a significant decrease in liver weight ($p < 0.0001$) compared with control rats.

The relative weights of organs in the malnutrition modeling group with a low-protein diet and enteropathy, and *A. paniculata* treatment were also evaluated. Rats in 2%LP+IND+AP1, 2%LP+IND+AP2, and 2%LP+IND+AP3 groups showed significant differences ($p < 0.05$) in the spleen and liver compared with the Control' and 2%LP+IND' groups (Figures 2A and 2B). At the end of the malnutrition model, the 2%LP+IND' rats demonstrated a WA of 48.4% (Table 2). The decrease in WA value indicated that the 2%LP+IND' diet resulted in severe malnutrition.

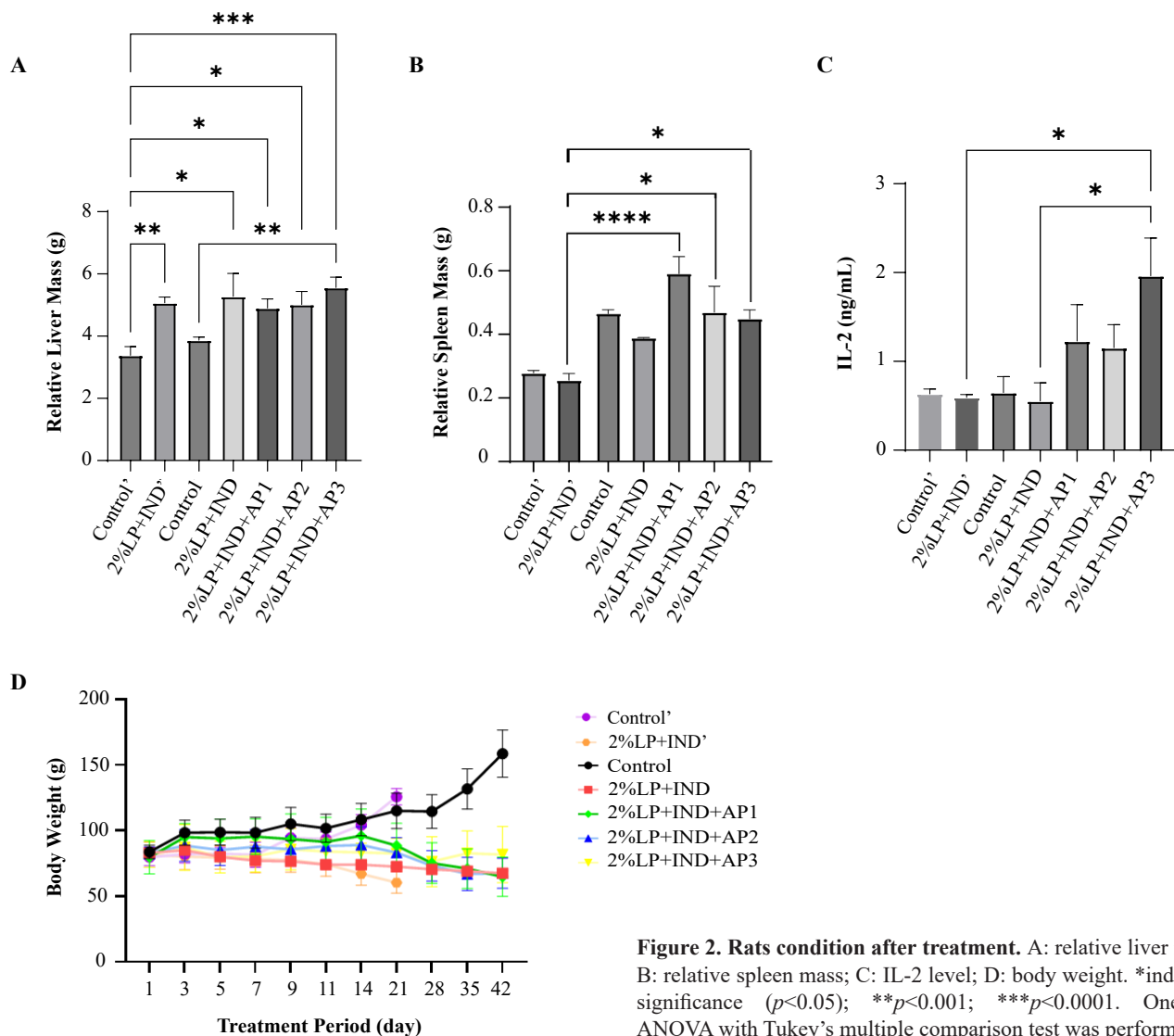


Figure 2. Rats condition after treatment. A: relative liver mass; B: relative spleen mass; C: IL-2 level; D: body weight. *indicates significance ($p < 0.05$); ** $p < 0.001$; *** $p < 0.0001$. One-way ANOVA with Tukey's multiple comparison test was performed.

Table 2. WA value for Control and 2%LP+IND groups.

Groups	WA values (%)				
	Day 1	Day 3	Day 7	Day 14	Day 21
Control'	63.9	65.7	65.4	83.5	101.0
2%LP+IND'	65.4	64.3	62.7	56.7	48.4
<i>p</i> -value	0.0853	0.5325	0.2133	<0.0001***	<0.0001***

APPLE Administration Increased Cholesterol, Glucose and Decreased Triglyceride

Significant differences were found in erythrocytes, hemoglobin, hematocrit, leukocyte, albumin, total protein, triglycerides, cholesterol, and glucose levels among all groups ($p < 0.05$). Administration of APPLE has not been able to significantly improve levels of erythrocytes, hemoglobin, hematocrit, leukocytes, albumin, and total protein. Post-hoc analysis revealed that administration of APPLE at a dose of 94.5 mg/kgBW in 2%LP+IND+AP2 group significantly increased cholesterol levels compared to the 2%LP+IND+AP1 and 2%LP+IND+AP3 ($p < 0.05$). Additionally, glucose levels increased and triglyceride levels decreased at dose of 189 mg/kgBW compared to those in the groups receiving 47.25 and 94.5 mg/kg BW (Table 3).

APPLE Administration Increased IL-2 Level

The lowest IL-2 level was found in 2%LP+IND group, with a value of 0.5530 ± 0.2060 ng/mL, whereas the highest was found in 2%LP+IND+AP3 group, with a value of 1.963 ± 0.4260 ng/mL. Post-hoc analysis showed that administration of APPLE for 21 days at a dose of 189 mg/kgBW to malnourished rats significantly increased IL-2 levels compared with the control group (Figure 2C).

APPLE Administration Increased Villus Height

Measurement of villous length and crypt depth in jejunum rats with malnutrition was performed to assess intestinal damage. The *A. paniculata* treatment group showed an increase in villus height in the 2%LP+IND+AP3 group compared to the 2%LP+IND group ($p < 0.05$) (Figure 3). The *A. paniculata* treatment did not have any noticeable impact on crypt depth (Table 4).

Discussion

In many cases, animal models of malnutrition are required to understand how malnutrition affects the course of the disease. (22) Many studies have used these models to assess how

malnutrition affects the immune system, other malnutrition-related illnesses, and susceptibility to infectious infections. (23) Our controlled analysis of the dietary characteristics of model animals was made possible by these features. Much of the literature employs low-protein, isocaloric diets that can mimic a type of protein malnutrition. (24) However, it is common for children living in precarious conditions to consume diets with both calorie and protein restrictions. (11) Therefore, in this study, a feeding protocol using a diet with low-protein contents was used.

Three days after the introduction of the low-protein diet, weanling Wistar rats showed a noticeable decrease in weight, which persisted until day 42 when the trial ended. This diet-induced severe and moderate malnutrition in rats. Marasmic malnutrition is a disease that results in numerous physical abnormalities, including significant loss of body weight, muscular mass, and subcutaneous fat, in addition to sluggish development, irritability, and lethargy. (25) Malnourished rats displayed a delay in body growth.

Atrophy of essential organs such as the pancreas, liver, spleen, and lymphoid tissues can result from marasmus. (3,25) This process results in a decrease in neutrophil phagocytic activity and T-cell production, and impairment in the generation of antibodies (4,8), which consequently increases the likelihood of infection (25).

The livers and spleens were weighed 42 days after the diet was introduced to evaluate the effects of starvation on internal organs. Malnourished rats showed a decrease in spleen weight compared to controls. Interestingly, starved rats had higher liver weights. Fatty liver and hepatomegaly are prevalent in kwashiorkor. (3,26) However, children with marasmus have been reported to exhibit hepatic steatosis and hepatomegaly. (27)

Hematological measurements showed that leukocyte counts were decreased in Wistar rats fed a low-protein diet. Malnutrition diagnosis also uses biochemical indicators. These include albumin, creatinine, total cholesterol, urea, and total lymphocyte count, which indicate inflammation. (12,28) Biochemical measurement showed that albumin, total protein, cholesterol, and glucose decreased in Wistar

Table 3. Hematological and biochemical parameters in all treatment groups.

Groups	Control'	2%LP+ IND'	Control	2%LP+IND	2%LP+IND+ API	2%LP+IND+ AP2	2%LP+IND+ AP3	p-value
Erythrocyte ($\times 10^3/\mu\text{L}$)	7.075 \pm 0.51	4.32 \pm 0.49*	6.59 \pm 0.31	4.94 \pm 0.95*	5.40 \pm 0.46	5.76 \pm 0.37	5.46 \pm 0.50*	0.0012**
Hemoglobin (g/dL)	13.54 \pm 0.37	7.70 \pm 0.69***	12.57 \pm 0.08	9.40 \pm 0.60	9.37 \pm 0.31*	10.57 \pm 0.92	9.40 \pm 0.59*	<0.0001***
Hematocrit (%)	46.34 \pm 3.17	22.06 \pm 2.71*	35.14 \pm 1.57	27.50 \pm 3.40	30.15 \pm 2.47**	31.45 \pm 3.05*	29.98 \pm 2.49	0.0001***
Leukocyte ($\times 10^6/\mu\text{L}$)	6.60 \pm 0.52	3.45 \pm 0.52*	7.52 \pm 2.13	4.80 \pm 0.80	5.82 \pm 0.90	2.10 \pm 0.10**	5.26 \pm 0.33	0.0020**
Albumin (mg/dL)	2.75 \pm 0.15	1.42 \pm 0.12***	2.23 \pm 0.07	1.86 \pm 0.04*	1.47 \pm 0.08*	2.22 \pm 0.28	2.19 \pm 0.16	0.0001***
Total Protein (mg/dL)	6.27 \pm 0.16	4.47 \pm 0.44*	6.01 \pm 0.29	4.80 \pm 0.09	4.15 \pm 0.06*	5.27 \pm 0.41	5.27 \pm 0.41	0.0020**
ALT (U/L)	42.08 \pm 2.51	38.30 \pm 2.71	46.80 \pm 4.00	36.45 \pm 0.55	48.53 \pm 2.81	41.03 \pm 3.82	39.35 \pm 0.65	0.1282
Triglyceride (mg/dL)	53.00 \pm 3.79	53.20 \pm 5.56	48.00 \pm 3.89	63.00 \pm 12.00	43.75 \pm 4.27	41.50 \pm 3.50	30.75 \pm 8.30*	0.0465*
Cholesterol (mg/dL)	48.40 \pm 5.62	31.40 \pm 2.22*	46.40 \pm 4.01	31.50 \pm 3.50	37.80 \pm 3.41	50.50 \pm 5.34*	49.50 \pm 3.20	0.0115*
Glucose (mg/dL)	133.80 \pm 8.04	111.50 \pm 6.24	143.00 \pm 14.58	101.50 \pm 4.50	100.80 \pm 7.47	114.50 \pm 12.39	141.00 \pm 8.28*	0.0234*

Signifies significance, * p <0.05; ** p <0.001; *** p <0.0001.

Table 4. Villi length and crypt depth in the jejunum of the malnutrition modeling and Andrographis paniculata treatment group.

Variable	Control'	2%LP+ IND'	Control	2%LP+IND	2%LP+IND+ API	2%LP+IND+ AP2	2%LP+IND+ AP3	p-value
Villi length (μm)	441.90 \pm 39.90	212.00 \pm 24.90	503.30 \pm 81.30	208.30 \pm 2.06	235.50 \pm 30.66	300.80 \pm 38.93	349.00 \pm 22.86**	0.0004***
Crypt depth (μm)	150.00 \pm 11.45	96.31 \pm 5.88	174.90 \pm 32.20	95.05 \pm 3.74	94.35 \pm 9.13	96.16 \pm 4.63	131.10 \pm 29.44	0.0615

Signifies significance, ** p <0.001; *** p <0.0001.

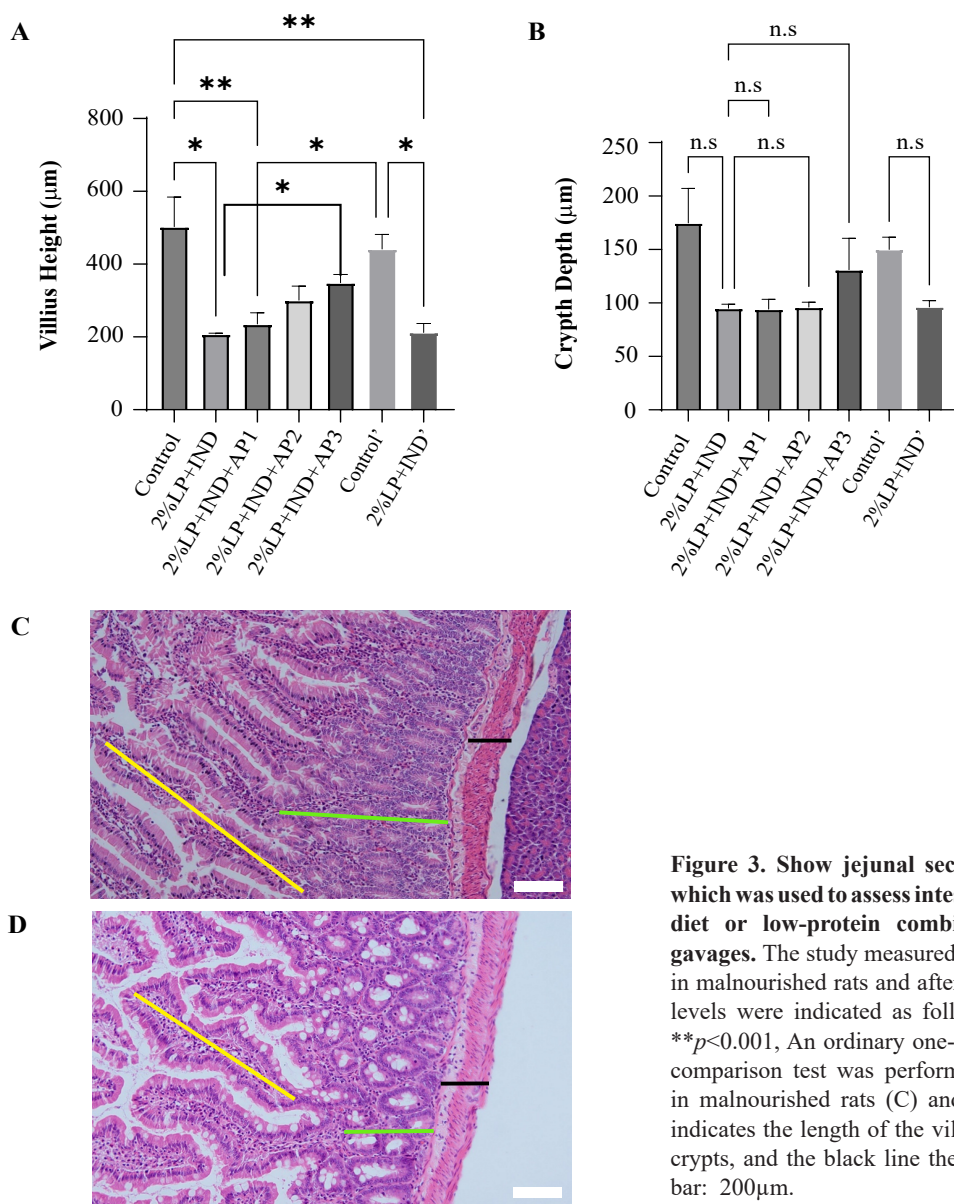


Figure 3. Show jejunal sections, stained with HES solution, which was used to assess intestinal damage in rats fed a standard diet or low-protein combined with chronic indomethacin gavages. The study measured villi length (A), and crypt depth (B) in malnourished rats and after treatment with APLE. Significance levels were indicated as follows: n.s.: not significant; * $p < 0.05$; ** $p < 0.001$. An ordinary one-way ANOVA with Tukey’s multiple comparison test was performed. The measurements were taken in malnourished rats (C) and control rats (D). The yellow line indicates the length of the villous, the green line the depth of the crypts, and the black line the thickness of the muscularis. White bar: 200µm.

rats fed a low-protein diet and APLE increased cholesterol and glucose.

To investigate the pathological mechanisms underlying enteropathy, researchers employ experimental models of enteropathy induced by chemical agents, such as indomethacin. The utilization of indomethacin allows for the manifestation of various symptoms associated with enteropathy, although it may not precisely replicate the same mechanisms implicated in the development of enteropathy. (29,30) Moreover, the use of indomethacin provides a straightforward and replicable model that elicits a controlled inflammatory response, which may be comparable to the subclinical symptoms observed in the pathophysiology of human enteropathy. Similar to the model established

by (31), which involves a low-protein diet and bacterial challenge, the current model effectively recapitulates key aspects of human enteropathy, including impaired growth, intestinal inflammation, and overall inflammation.

The murine model of undernutrition exhibits both intestinal inflammation and hyperpermeability, two characteristics that closely resemble those observed in enteropathy, particularly in young children under the age of five who experience severe wasting either before or after significant linear growth retardation occurs.

The active compound in *A. paniculata* is andrographolide which can act as an immunostimulant for specific and non-specific immune functions through natural killer (NK) cells, macrophages, and cytokine induction. It

will also send intracellular signals to cell receptors to increase their activity when immune system activity is reduced. This can increase the production of IL-2, thereby increasing lymphocyte proliferation, as well as the proliferation and differentiation of B and NK cells.(32)

IL-2, a pleiotropic cytokine, functions as an immunostimulator or immune inhibitor depending on the target cell. The main function of IL-2 is to regulate T-cell homeostasis and growth.(33,34) IL-2 activates anti-apoptotic mechanisms to prevent immune cell death.(35) Low doses of IL-2 are effective in modifying the gut microbiome against dysbiosis.(36-38) *A. paniculata* extract decreases inflammatory intestinal epithelial cells with its role as an antiparasitic and anti-inflammatory agent.(39) However, Administration of andrographolide caused an increase in the proportion and abundance of beneficial bacteria, and the intestinal microbial composition of Firmicutes dominated after andrographolide treatment.(40) While this study did not observe significant changes in hematological parameters, further research could be conducted to evaluate the effects of *A. paniculata* on hematological parameters in cases of malnutrition and enteropathy.

Conclusion

The administration of APLE to the malnourished group at a dose of 94.5 mg/kgBW increased cholesterol levels. Furthermore, at a dose of 189 mg/kgBW, it increased IL-2 levels, glucose levels, and villi length. Additionally, it decreased triglyceride levels. The administration of APLE may improve nutrition and reduce the risk of malnutrition due to immune disorders related to a low-protein diet and enteropathy.

Acknowledgments

This research was supported by the Ministry of Health Republic of Indonesia (No. HK.03.01/2/05702/2021). The authors would like to thank the Disease Investigation Center (DIC) in Banjarbaru Indonesia for their assistance in facilitating research laboratories, CV. Indonegri, Malang, West Jawa, Indonesia for helping in the manufacture of *Andrographis paniculata* extracts, the Laboratory of Animal Nutrition, Department of Animal Science, Faculty of Agriculture, Lambung Mangkurat University were formulated experimental diets.

Authors Contribution

FD, RN, and I were involved in concepting and planning the research, FD performed the data collection, calculated the experimental data and performed the analysis, FD, RN and I drafted the manuscript, designed the figures and interpreting the results. RN, I, IY and S were involved in giving critical revision of the manuscript.

References

1. Arthur SS, Nyide B, Soura AB, Kahn K, Weston M, Sankoh O. Tackling malnutrition: A systematic review of 15-year research evidence from INDEPTH health and demographic surveillance systems. *Glob Health Action*. 2015; 8: 28298. doi: 10.3402/gha.v8.28298.
2. UNICEF/WHO/WORLD BANK. Levels and Trends in Child Malnutrition: UNICEF/WHO/World Bank Group Joint Child Malnutrition Estimates: Key Findings of The 2023 Edition. New York: World Health Organization; 2023.
3. Michael H, Amimo JO, Rajashekara G, Saif LJ, Vlasova AN. Mechanisms of kwashiorkor-associated immune suppression: Insights from human, mouse, and pig studies. *Front Immunol*. 2022; 13: 826268. doi: 10.3389/fimmu.2022.826268.
4. Bourke CD, Berkley JA, Prendergast AJ. Immune dysfunction as a cause and consequence of malnutrition. *Trends Immunol*. 2016; 37(6): 386-98.
5. Bhutta ZA, Berkley JA, Bandsma RHJ, Kerac M, Trehan I, Briend A. Severe childhood malnutrition. *Nat Rev Dis Prim*. 2017; 3: 17067. doi: 10.1038/nrdp.2017.67.
6. Takele Y, Adem E, Getahun M, Tajebe F, Kiflie A, Hailu A, et al. Malnutrition in healthy individuals results in increased mixed cytokine profiles, altered neutrophil subsets and function. *PLoS One*. 2016; 11(8): e0157919. doi: 10.1371/journal.pone.0157919.
7. Bourke CD, Jones KDJ, Prendergast AJ. Current understanding of innate immune cell dysfunction in childhood undernutrition. *Front Immunol*. 2019; 10: 1728. doi: 10.3389/fimmu.2019.01728.
8. Alwarawrah Y, Kiernan K, MacIver NJ. Changes in nutritional status impact immune cell metabolism and function. *Front Immunol*. 2018; 9: 1055. doi: 10.3389/fimmu.2018.01055.
9. Budge S, Parker AH, Hutchings PT, Garbutt C. Environmental enteric dysfunction and child stunting. *Nutr Rev*. 2019; 77(4): 240-53.
10. Tickell KD, Atlas HE, Walson JL. Environmental enteric dysfunction: A review of potential mechanisms, consequences and management strategies. *BMC Med*. 2019; 17(1): 181. doi: 10.1186/s12916-019-1417-3.
11. Salameh E, Jarbeau M, Morel FB, Zeilani M, Aziz M, Déchelotte P, et al. Modeling undernutrition with enteropathy in mice. *Sci Rep*. 2020; 10: 15581. doi: 10.1038/s41598-020-72705-0.
12. Bharadwaj S, Ginoya S, Tandon P, Gohel TD, Guirguis J, Vallabh H, et al. Malnutrition: Laboratory markers vs nutritional assessment. *Gastroenterol Rep*. 2016; 4(4): 272-80.
13. Santos EW, Oliveira DC, Silva GB, Tsujita M, Beltran JO, Hastreiter A, et al. Hematological alterations in protein malnutrition. 2017; 75(11): 909-19.

14. González-Torres C, González-Martnez H, Miliar A, Nájera O, Graniel J, Firo V, *et al.* Effect of malnutrition on the expression of cytokines involved in Th1 cell differentiation. *Nutrients*. 2013; 5(2): 579–93.
15. Goudet SM, Griffiths PL, Bogin BA, Madise NJ. Nutritional interventions for preventing stunting in children (0 to 5 years) living in urban slums in low and middle-income countries (LMIC) (Protocol). *Cochrane Libr*. 2015; 2015 (5): 1–44. doi: 10.1002/14651858.CD011695.
16. Kevin M, Widyastiti NS, Budijitno S, Prajoko YW, Susilaningih N. The protective effect of *Andrographis paniculata* against lipopolysaccharide-induced sepsis in lung tissues of a rat model through the decrease of ICAM-1 and E-selectin expression. *Indones Biomed J*. 2023; 15(6): 411–9.
17. Chao WW, Lin BF. Isolation and identification of bioactive compounds in *Andrographis paniculata* (Chuanxinlian). *Chin Med*. 2010; 5: 17. doi: 10.1186/1749-8546-5-17.
18. Xiang DC, Yang JY, Xu YJ, Zhang S, Li M, Zhu C, *et al.* Protective effect of *Andrographolide* on 5-Fu induced intestinal mucositis by regulating p38 MAPK signaling pathway. *Life Sci*. 2020; 252: 117612. doi: 10.1016/j.lfs.2020.117612.
19. Churiyah, Pongtuluran, Rofaani E, Tarwadi. Antiviral and immunostimulant activities of *Andrographis paniculata*. *Hayati J Biosci*. 2015; 22(2): 67–72.
20. National Research Council (US) Subcommittee on Laboratory Animal Nutrition. *Nutrient Requirements of Laboratory Animals: Fourth Revised Edition, 1995*. Washington (DC): National Academies Press (US); 1995.
21. Anstead GM, Chandrasekar B, Zhao W, Yang J, Perez LE, Melby PC. Malnutrition alters the innate immune response and increases early visceralization following *Leishmania donovani* infection. *Infect Immun*. 2001; 69(8): 4709–18.
22. Ibrahim MK, Zambruni M, Melby CL, Melby PC. Impact of childhood malnutrition on host defense and infection. *Clin Microbiol Rev*. 2017; 30(4): 919–71.
23. Walson JL, Berkley JA. The impact of malnutrition on childhood infections. *Curr Opin Infect Dis*. 2018; 31(3): 231–6.
24. Salameh E, Morel FB, Zeilani M, Déchelotte P, Marion-Letellier R. Animal models of undernutrition and enteropathy as tools for assessment of nutritional intervention. *Nutrients [Internet]*. 2019; 11(9): 2233. doi: 10.3390/nu11092233.
25. Pham TPT, Alou MT, Golden MH, Million M, Raoult D. Difference between kwashiorkor and marasmus: Comparative meta-analysis of pathogenic characteristics and implications for treatment. *Microb Pathog*. 2021; 150: 104702. doi: 10.1016/j.micpath.2020.104702.
26. Estrela D, Federal U, Guimar TB. Effects of short-term malnutrition in rats. *Sci Plena*. 2014; 10: 071101.
27. Ferreira-Paes T, Seixas-Costa P, Almeida-Amaral EE. Validation of a feed protocol in a mouse model that mimics marasmic malnutrition. *Front Vet Sci*. 2021; 8: 757136. doi: 10.3389/fvets.2021.757136.
28. Zhang Z, Pereira SL, Luo M, Matheson EM. Evaluation of blood biomarkers associated with risk of malnutrition in older adults: A systematic review and meta-analysis. *Nutrients*. 2017; 9(8): 829. doi: 10.3390/nu9080829.
29. Xiao X, Nakatsu G, Jin Y, Wong S, Yu J, Lau JYW. Gut microbiota mediates protection against enteropathy induced by indomethacin. *Sci Rep*. 2017; 7: 40317. doi: 10.1038/srep40317.
30. Sugimura N, Otani K, Watanabe T, Nakatsu G, Shimada S, Fujimoto K, *et al.* High-fat diet-mediated dysbiosis exacerbates NSAID-induced small intestinal damage through the induction of interleukin-17A. *Sci Rep*. 2019; 9(1): 4–6.
31. Brown EM, Wlodarska M, Willing BP, Vonaesch P, Han J, Reynolds LA, *et al.* Diet and specific microbial exposure trigger features of environmental enteropathy in a novel murine model. *Nat Commun [Internet]*. 2015; 6: 7806. doi: 10.1038/ncomms8806.
32. Sheeja K, Kuttan G. Modulation of natural killer cell activity, antibody-dependent cellular cytotoxicity, and antibody-dependent complement-mediated cytotoxicity by *andrographolide* in normal and Ehrlich ascites carcinoma-bearing mice. *Integr Cancer Ther*. 2007; 6(1): 66–73.
33. Pol JG, Caudana P, Paillet J, Piaggio E, Kroemer G. Effects of interleukin-2 in immunostimulation and immunosuppression. *J Exp Med*. 2020; 217(1): e20191247. doi: 10.1084/jem.20191247.
34. Ross SH, Cantrell DA. Signaling and function of interleukin-2 in T lymphocytes. *Annu Rev Immunol*. 2018; 36: 411–33.
35. Cortés-Barberena E, González-Márquez H, Gómez-Olivares JL, Ortiz-Muñiz R. Effects of moderate and severe malnutrition in rats on splenic T lymphocyte subsets and activation assessed by flow cytometry. *Clin Exp Immunol*. 2008; 152(3): 585–92.
36. Li N, Li X, Su R, Wu R, Niu HQ, Luo J, *et al.* Low-dose interleukin-2 altered gut microbiota and ameliorated collagen-induced arthritis. *J Inflamm Res*. 2022; 15(February): 1365–79.
37. Tchitchek N, Tchoumba ON, Pires G, Dandou S, Campagne J, Churlaud G, *et al.* Low-dose IL-2 shapes a tolerogenic gut microbiota that improves autoimmunity and gut inflammation. *JCI Insight*. 2022; 7(17): e159406. doi: 10.1172/jci.insight.159406.
38. Zhufeng Y, Xu J, Miao M, Wang Y, Li Y, Huang B, *et al.* Modification of intestinal microbiota dysbiosis by low-dose interleukin-2 in dermatomyositis: A post hoc analysis from a clinical trial study. *Front Cell Infect Microbiol*. 2022; 12: 757099. doi: 10.3389/fcimb.2022.757099.
39. Ardika RG, Budiono BP, Widiastiti NS, Maharani N, Sysilaningih N, Sandra F. *Andrographis paniculata* leaves extract inhibit TNF- α and caspase-3 expression of septic rats' intestinal tissues *ryco*. *Indones Biomed J*. 2024; 16(1): 66–71.
40. Wu H, Wu X, Huang L, Ruan C, Liu J, Chen X, *et al.* Effects of *andrographolide* on mouse intestinal microflora based on high-throughput sequence analysis. *Front Vet Sci*. 2021; 8: 702885. doi: 10.3389/fvets.2021.702885.